Title

Emergent Coordination of the CHKB and CPT1B Genes in Eutherian Mammals: Implications for the Origin of Brown Adipose Tissue

Journal

Journal of Molecular Biology, 432(23)

ISSN

0022-2836

Authors

Patel, Bhavin V
Yao, Fanrong
Howenstine, Aidan
et al.

Publication Date

2020-11-01

DOI

10.1016/j.jmb.2020.09.022

Peer reviewed

HHS Public Access

Author manuscript

J Mol Biol. Author manuscript; available in PMC 2021 November 20.

Published in final edited form as:

J Mol Biol. 2020 November 20; 432(23): 6127–6145. doi:10.1016/j.jmb.2020.09.022.

Emergent Coordination of the *CHKB* and *CPT1B* Genes in Eutherian Mammals: Implications for the Origin of Brown Adipose Tissue

Bhavin V. Patel[1], **Fanrong Yao**[1], **Aidan Howenstine**[2], **Risa Takenaka**[2], **Jacob A. Hyatt**[1], **Karen E. Sears**[2], **Brian M. Shewchuk**[1,*]

[1]Department of Biochemistry & Molecular Biology, Brody School of Medicine, East Carolina University, Greenville, NC 27834

[2]Department of Ecology & Evolutionary Biology, College of Life Sciences, University of California Los Angeles, Los Angeles, CA 90095

Abstract

Mitochondrial fatty acid oxidation (FAO) contributes to the proton motive force that drives ATP synthesis in many mammalian tissues. In eutherian (placental) mammals, brown adipose tissue (BAT) can also dissipate this proton gradient through uncoupling protein 1 (UCP1) to generate heat, but the evolutionary events underlying the emergence of BAT are unknown. An essential step in FAO is the transport of cytoplasmic long-chain acyl-coenzyme A (acyl-CoA) into the mitochondrial matrix, which requires the action of carnitine palmitoyltransferase 1B (CPT1B) in striated muscle and BAT. In eutherians, the *CPT1B* gene is closely linked to the *choline kinase beta* (*CHKB*) gene, which is transcribed from the same DNA strand and terminates just upstream of *CPT1B*. CHKB is a rate-limiting enzyme in the synthesis of phosphatidylcholine (PC), a predominant mitochondrial membrane phospholipid, suggesting that the coordinated expression of *CHKB* and *CPT1B* may cooperatively enhance mitochondrial FAO. The present findings show that transcription of the eutherian *CHKB* and *CPT1B* genes is linked within a unitary epigenetic domain targeted to the *CHKB* gene, and that that this regulatory linkage appears to have resulted from an intergenic deletion in eutherians that significantly altered the distribution of *CHKB* and *CPT1B* expression. Informed by the timing of this event relative to the emergence of BAT, the

*Corresponding author: Brian M. Shewchuk, Ph.D., Department of Biochemistry & Molecular Biology, Brody School of Medicine at East Carolina University, 600 Moye Blvd., Greenville, NC 27834, shewchukb@ecu.edu, (252) 744-5096.

Patel *et al.* credit author statement

BVP: Conceptualization, Methodology, Investigation, Writing – Original Draft, Writing – Review & Editing
FY: Methodology, Investigation, Writing – Original Draft, Writing – Review & Editing
AH: Resources, Investigation
RT: Resources, Investigation
JAH: Investigation
KES: Resources, Writing – Review & Editing
BMS: Conceptualization, Methodology, Investigation, Writing – Original Draft, Writing – Review & Editing

Declaration of interests

The authors declare that they have no known competing financial interests or personal relationships that could have appeared to influence the work reported in this paper.

phylogeny of *CHKB-CPT1B* synteny, and the insufficiency of UCP1 to account for eutherian BAT, these data support a mechanism for the emergence of BAT based on the acquisition of a novel capacity for adipocyte FAO in a background of extant UCP1.

Graphical abstract

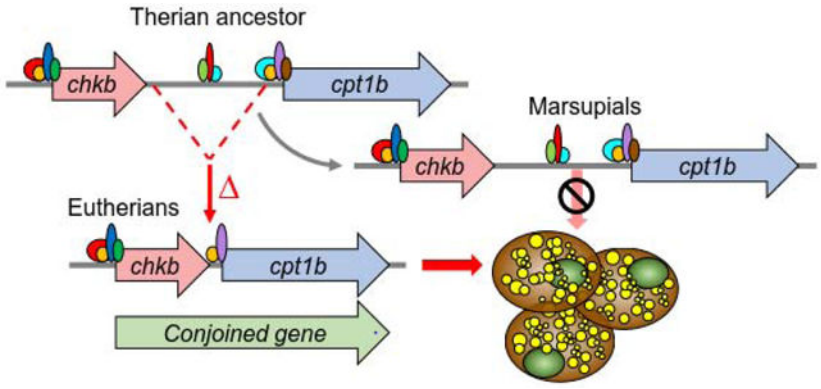

Keywords

Brown adipose tissue; CHKB; CPT1B; fatty acid oxidation; conjoined gene

Introduction

Lipid metabolism contributes significantly to homeostasis in mammals and is regulated at multiple levels in response to diet, stress, physical activity, reproduction, and the environment. The mitochondrial β-oxidation of long chain fatty acids derived from both dietary lipids and triglycerides synthesized *de novo* is the predominant pathway for the generation of ATP from lipids. Fatty acid oxidation (FAO) produces NADH and $FADH_2$ both directly and through the complete oxidation of the acetyl-coenzyme A (acetyl-CoA) product in the TCA cycle. The oxidation of NADH and $FADH_2$ in turn generates a proton motive force that fuels ATP synthesis in a broad range of tissues which spares systemic glucose, and tissues like striated muscle rely heavily on FAO to provide enough ATP for the elevated demand in these cells. In brown adipose tissue (BAT), the FAO derived proton flux also fuels the thermogenic leakage of protons back into the mitochondrial matrix through inner membrane localized uncoupling protein 1 (UCP1), which contributes significantly to thermoregulation uniquely in eutherian (placental) mammals.

A rate-limiting reaction in the pathway for FAO is the synthesis of acylcarnitine from cytoplasmic long chain fatty acyl-CoA as required for transport into the mitochondrial matrix for β-oxidation [1]. The exchange of the CoA moiety for carnitine is mediated by carnitine palmitoyltransferase 1 (CPT1), which exists as three independently encoded isoforms with differing tissue predominance: the liver isoform CPT1A expressed in many non-muscle tissues, the muscle isoform CPT1B expressed in striated muscle and BAT, and the brain isoform CPT1C. As skeletal muscle represents a major site of FAO, regulation of the *CPT1B* gene has been a focus of research on the systemic control of lipid metabolism

and its derangement in metabolic disease. *CPT1B* is regulated by long chain fatty acid levels and other signals that govern FAO in skeletal muscle congruent with substrate availability and energetic needs, which is mediated at the gene level through multiple characterized gene-proximal elements [2–14]. Perhaps significantly, the regulation of *CPT1B* transcription by proximal complexes occurs in the vicinity of an additional gene transcribed from the same DNA strand that terminates just a few hundred nucleotides upstream of *CPT1B* and encodes choline kinase beta (CHKB), a rate limiting enzyme in the CDP-choline pathway (Kennedy pathway) for phosphatidylcholine (PC) biosynthesis (Figure 1a) [15–17]. However, little is known about the regulation of the *CHKB* gene [18].

The significance of CPT1B activity in homeostasis is illuminated by the phenotype of homozygous CPT1B knockout (*Cpt1b*$^{-/-}$) mice, which die *in utero* before embryonic day 9.5–11.5 [19]. An absolute requirement for CPT1B expression is corroborated by the lack of severe *CPT1B* mutations in humans. However, a common *CPT1B* haplotype is associated with multiple markers of metabolic syndrome, consistent with the importance of CPT1B activity in maintaining metabolic homeostasis [20]. Previous studies demonstrated that a normal upregulation of the *CPT1B* gene in response to fatty acids observed in primary human skeletal myotube cultures was blunted in association with obesity, accompanied by repressive epigenetic changes and shifts in transcription factor occupancy at the *CPT1B* gene, and a reduction in cellular FAO [10, 21]. It was concluded from these findings that part of the basis for the positive lipid balance associated with obesity is the stable epigenetic programming of the *CPT1B* gene in the obesogenic environment, which reduces its capacity for lipid-mediated activation, and that changes in *CPT1B* expression can affect cellular oxidative capacity. This model for an essential, rate-limiting role of CPT1B in skeletal muscle lipid metabolism that is relevant to metabolic disease has been reinforced in several experimental systems [19, 22, 23]. As such, the regulation of this gene locus continues to be an attractive target for approaches to modify FAO therapeutically, and to understand the regulation of lipid metabolism in physiology and disease more broadly.

Consistent with the elevated FAO capacity of BAT, brown adipocytes possess distinct mechanisms for endogenous lipid storage and catabolism. Unlike white adipocytes, which store triglycerides in a single large cytoplasmic lipid droplet from which fatty acids are released into circulation by hormone-activated lipases in response to fasting and stress, brown adipocyte triglycerides are stored in multilocular lipid droplets as a source of fatty acids to be oxidized endogenously in numerous mitochondria to fuel UCP1-mediated thermogenesis, largely in response to β-adrenergic signaling stimulated by cold exposure [24–27]. The elevated β-oxidation of fatty acids and resulting ATP synthesis can also fuel UCP1-independent thermogenesis in skeletal muscle in a mechanism involving the sarco/endoplasmic reticulum Ca^{2+}-ATPase (SERCA), indicating that the significance of FAO to non-shivering thermogenesis may extend beyond BAT [28–31].

In addition to UCP1 expression, and the enhanced lipolysis provided by multilocular lipid droplets, a defining parameter of the eutherian BAT phenotype is the elevated expression of genes associated with the oxidation of endogenously stored lipids to fuel thermogenesis. This is accompanied by the induction of mitochondrial biogenesis, collectively increasing the capacity for oxidative metabolism in BAT [24–27]. The activation of endogenous lipid

catabolism also occurs in ‘beige’ adipocytes, an inducible phenotype recruited from white adipose tissue (WAT) that attains BAT-like characteristics in response to certain stimuli. Because of their elevated FAO capacity, brown and beige adipocytes contribute to the depletion of systemic fat and are thus a target for therapeutic approaches to counter obesity [25, 32, 33]. Informatively, heterozygous CPT1B knockout mice, which display a 50% reduction in carnitine palmitoyltransferase activity specifically in skeletal muscle, heart, and BAT, die of fatal hypothermia following a three hour cold challenge [19], illuminating the significance of CPT1B activity in thermogenesis. Considering the similarities in the FAO functions of BAT and skeletal muscle, understanding the regulation of *CPT1B* in BAT would complement investigation of the *CPT1B* regulation in skeletal muscle in the context of thermoregulation and metabolic homeostasis.

Interestingly, despite its central function in eutherian non-shivering thermogenesis, UCP1 alone cannot account for the evolutionary emergence of BAT, as the functional UCP gene family (*UCP1*, *UCP2*, *UCP3*) has been extant since the bony fish common ancestor, with significant amino acid sequence identity among endothermic and ectothermic species. Furthermore, marsupials can acquire multilocular adipocytes that express UCP1 upon cold stimulation, suggesting that a pathway exists in marsupials to establish the framework for augmented adipocyte lipolysis and thermogenic proton leakage. However, marsupials cannot form thermogenic BAT despite the presence of functional UCP1 [34–39]. Indeed, phylogenetic analysis of UCP1 amino acid sequences among eutherian and non-eutherian species has confirmed that UCP1 has undergone neutral evolution, displaying no purifying adaptive changes in eutherians and supporting the observation that the biochemical properties of UCP1 in endothermic and ectothermic species are likely the same, mediating proton flux in common nonthermogenic processes [40, 41]. These observations show that UCP1 is necessary but not sufficient for canonical eutherian BAT and suggest that what had yet to evolve in the eutherian ancestor was a mechanism for enhanced endogenous mitochondrial FAO in extant cold-stimulated multilocular adipocytes that could supply UCP1-mediated proton flux at thermogenic levels [40].

In the present study, we expand the analysis of *CPT1B* gene regulation, informed by its central rate-limiting activity in striated muscle and BAT FAO. Specifically, we address the role that the closely apposed *CHKB* gene may play in the regulation of *CPT1B*. Beyond the potential for a transcriptional regulatory interaction due to their genomic proximity, a primary impetus for this study is the potential for the *CHKB* and *CPT1B* gene products to cooperatively reinforce cellular FAO. As mentioned above, CHKB is a rate-limiting enzyme in the synthesis of PC, a major membrane phospholipid and the predominant phospholipid comprising the inner mitochondrial membrane. Consistent with this essential function, both naturally occurring *CHKB* alleles in humans and induced mutations of *Chkb* in mice result in a megaconial mitochondrial muscular dystrophy due specifically to a deficiency of PC [42–49]. Thus, an upregulation of CHKB has the potential to increase PC availability for mitochondrial membrane synthesis, which could reinforce mitochondrial FAO in concert with an increase in CPT1B protein levels such that the coordinated expression of the *CHKB* and *CPT1B* genes plays an important role in maintaining cellular FAO levels in muscle and BAT. The findings presented here show that the expression of the *CHKB* and *CPT1B* genes is linked within a unitary domain of histone modifications and RNA polymerase II

(RNAPII) transcription initiation targeted to the *CHKB* gene, and that this transcriptional and epigenetic linkage appears to have resulted from an intergenic deletion that occurred at the point of marsupial/eutherian divergence in mammalian evolution. Informed by the timing of this event relative to the emergence of BAT, the phylogeny of the *chkb-cpt1b* linkage, and the inability of functional changes in extant UCP1 to account for the acquisition of the eutherian BAT phenotype, these data support an evolutionary path for the emergence of BAT and homeothermy in eutherian mammals based on the serendipitous acquisition of a novel capacity for adipocyte FAO in a background of extant functional UCP1.

Results and Discussion

Transcription of the *Chkb* and *Cpt1b* genes is coordinated in mice.

As noted above, a series of early transfection studies identified several transcription factors that affect *CPT1B* transcription through proximal elements. However, the regulation of *CPT1B* in its natural chromatin locus *in vivo* has not been well examined, particularly in the context of the regulation of the nearby *CHKB* gene (Figure 1a). One possible outcome of the close apposition of the *CHKB* and *CPT1B* genes is an overlap in the *cis*-acting regulatory domains of the two genes, such that their transcription is linked by a common regulatory mechanism that controls the expression of both genes in concert. Spliced readthrough fusion transcripts that contain exons from both *CHKB* and *CPT1B* are readily observable in both mice and humans [50, 51], indicative of a potential transcriptional coincidence. In order to assess the coordinated regulation of the *Chkb* and *Cpt1b* genes, transcripts were measured in mouse tissues to determine whether they are transcribed in concert. As shown in Figure 2a, both genes are transcribed at a notably high level in BAT, followed by moderate relative levels in skeletal muscle and heart. The role of CPT1B in mediating a high capacity for FAO in these tissues has been established and is consistent with the unique demand. In contrast, they were both transcribed at low levels in WAT where FAO is limited, and liver, where CPT1A is the predominant CPT1 isoform. The *Chkb-Cpt1b* fusion transcript showed the same general distribution. The congruent tissue specificities of the *Cpt1b* and *Chkb* genes indicates the potential for the coordinated transcriptional regulation of these genes and suggests that *Chkb* and *Cpt1b* expression support a common process. In particular, the highest expression levels of both genes in BAT suggests that the coordinated expression of these genes may be especially relevant in this tissue. Immunoblot analysis of mouse tissues lysates corroborated the transcript levels, showing the highest CPT1B protein levels in BAT, followed by skeletal muscle and heart (Figure 2b). The distribution of the additional fatty acid translocation pathway enzyme transcripts, *carnitine-acylcarnitine translocase (Slc25a20)* and *carnitine palmitoyltransferase 2 (Cpt2)*, were congruent with the relative levels of *Chkb* and *Cpt1b*, corroborating the elevated capacity for FAO in heart, skeletal muscle and BAT (Figure 2a).

The *CPT1B* gene is regulated by long chain fatty acids as ligands for peroxisome proliferator-activated receptors (PPAR) that transactivate the *CPT1B* gene through fatty acid response elements (FARE) in the *CPT1B* proximal 5’-flanking region [2, 3, 6]. In order to further test whether regulation of the *CHKB* and *CPT1B* genes is coordinated, the effects of palmitate exposure on *Chkb* and *Cpt1b* transcript levels in cultured mouse myotubes was

determined. As shown in Figure 2c, *Chkb* and *Cpt1b* mRNA levels increased in parallel in C2C12 myotubes in response to palmitate. These results indicate that transcription of the *Chkb* and *Cpt1b* genes can be regulated in concert by fatty acids, consistent with a regulatory linkage due to their genomic apposition. The level of the fusion transcript was also responsive to palmitate. These results, showing coordinated regulation and the formation of a spliced *Chkb-Cpt1b* fusion transcript, meet the operational classification of a 'conjoined' gene, a recognized phenomenon predicted at several hundred loci in the human genome [52–54].

The mouse *Chkb* and *Cpt1b* genes are encompassed in a unitary domain of histone modification and RNA polymerase II initiation targeted to the *Chkb* gene.

Gene activation and repression are mechanistically linked to specific chromatin modifications that contribute to the establishment and maintenance of gene activity states. In addition to DNA methylation, these epigenetic mechanisms involve nucleosomal histone modifications that have structural and cofactor recruitment functions in modulating gene activity [55, 56]. Of these modifications, the acetylation of histone 3 (H3) and histone 4 (H4) at multiple lysine residues alters electrostatic interactions leading to a more transcriptionally permissive chromatin state, and also functions to recruit nucleosome remodeling complexes. Histone acetyltransferases (HATs) are recruited to genes by DNA-binding transcription factors as components of coactivator complexes, and foci of histone acetylation above background levels are thus a marker for *cis*-acting regulatory sequences to which HAT activities are recruited, such as enhancers, promoters and transcription start sites. To map the pattern of histone acetylation across the contiguous *Chkb-Cpt1B* gene locus, a chromatin immunoprecipitation (ChIP) assay was performed with chromatin prepared from mouse C2C12 cell myotubes using a panacetyl-H3 antibody. Surprisingly, despite the parallel expression of the *Chkb* and *Cpt1b* genes, there was a single peak of histone acetylation at the 5' end of the *Chkb* gene (amplicons m3 and m4, Figure 1b), coincident with a known CpG island (CGI) [18] (Figure 3a). There was not a separate domain of histone acetylation targeted to the putative *Cpt1b* promoter, which indicates the possibility of a single *cis*-acting region at *Chkb* affecting the transcription of both genes in concert. A similar pattern of H3 acetylation was identified in differentiated primary mouse myotubes (Figure 3b), the mouse brown adipocyte cell line DE2.3 (Figure 3c) and differentiated primary mouse brown adipocytes (Figure 3d). These findings indicate that HAT activity is being recruited to a single site in the mouse *Chkb-Cpt1b* locus near the transcription start site of the *Chkb* gene in skeletal muscle and BAT.

In addition to histone lysine acetylation, foci of specific histone lysine methylation mediated by recruited histone methyltransferases are associated with domains of transcriptional activation. One such mark, H3 lysine 4 trimethylation (H3K4me3), is enriched around transcription start sites, and its distribution is informative in identifying sites of RNAPII initiation [56]. Similar to what was observed for histone acetylation, a ChIP assay of chromatin from mouse DE2.3 brown adipocytes using an antibody specific for H3K4me3 revealed a single peak at the *Chkb* gene (amplicon m3). No discrete peak of H3K4me3 was localized to a separate putative *Cpt1b* promoter. The colocalization of single foci of H3 hyperacetylation and H3K4me3 at the 5' end of the *Chkb* gene suggests that elements there

are recruiting coactivator complexes to regulate both the *Chkb* and *Cpt1b* genes, considering their coordinated transcription (Figure 2). These observations also raise the possibility that *Chkb* may serve as the predominant site of RNAPII transcription initiation that leads ultimately to the production of both *Chkb* and *Cpt1b* mRNA. Indeed, the readily detected spliced readthrough transcript that contains exons from both genes provides direct evidence for the processivity of RNAPII through both genes (Figure 2). In order to directly map the distribution of RNAPII transcription initiation throughout the *Chkb-Cpt1b* locus, a ChIP assay was performed using antibodies specific for the initiating (serine 5-phosphorylated) and elongating (serine 2-phosphorylated) forms of RNAPII with differentiated mouse DE2.3 brown adipocytes. The results indicated that the initiating serine 5-phosphorylated form of RNAPII was localized predominantly at the 5' end of *Chkb* (Figure 4b), while the elongating serine 2-phosphorylated form of RNAPII was distributed downstream in a continuous domain across both the *Chkb* and *Cpt1b* genes (Figure 4c). Significantly, there was not an independent peak of serine 5-phosphorylated RNAPII observed at the putative *Cpt1b* promoter, indicating a lack of independent transcription initiation there. Considered in conjunction with the patterns of histone modification, these data reinforce the possibility that the *Chkb* promoter and associated regulatory sequences are controlling the transcription of both the *Chkb* and *Cpt1b* genes. However, the responsiveness of *Chkb* to palmitate indicates that a reciprocal regulatory crosstalk may also result from the apposition, in light of the established fatty acid responsiveness of the proximal *Cpt1b* 5'-flanking region.

Considering the high level of mouse *Chkb* and *Cpt1b* transcription in BAT (Figure 2), it would be informative to determine if this locus is regulated by known mediators of the BAT phenotype. The transcriptional coactivator PRD1-BF1-RIZ1 homologous domain containing 16 (PRDM16) has a central function in controlling a bi-directional switch in cell fate between brown adipocytes and skeletal myoblasts in development. PRDM16 manifests this effect through the activation of a suite of BAT selective genes, while also repressing the expression of white adipocyte specific genes [57, 58]. The seminal role of PRDM16 in the establishment of the BAT lineage raises the question of whether the *Chkb-Cpt1b* locus is also a direct target of PRDM16 action. However, a ChIP assay for PRDM16 showed no evidence for localization to the *Chkb-Cpt1b* locus in mouse BAT or DE2.3 adipocytes (data not shown), suggesting that any involvement of PRDM16 in the regulation of this locus is likely indirect, mediated by downstream effectors of PRDM16 activity, or through elements beyond the genomic boundaries of the current analysis. Future studies will focus on the dynamics and molecular details of *Chkb-Cpt1b* locus regulation during brown adipocyte, white adipocyte, and myocyte ontogeny to address this question more rigorously.

A single domain of histone modification is targeted to the *CHKB* gene in primary human myotubes.

If the unitary epigenetic domain associated with conjoined *chkb* and *cpt1b* genes is functionally significant to FAO in muscle and BAT, the conservation of a tight intergenic distance in humans predicts that single foci of histone modifications targeted to *chkb* may be a common feature of eutherians. To begin to address this, primary human myoblasts were expanded and differentiated into myotubes *ex vivo*, and ChIP assays performed with acetyl-H3 and H3K4me3 antibodies. Single foci of H3 acetylation (Figure 5a) and H3 lysine 4

trimethylation (Figure 5b) were localized to the CGI at the 5' end of *CHKB* (amplicons h2 and h3, Figure 1), similar to the pattern observed in mice (Figure 3, 4). This result suggests that conjoined *chkb* and *cpt1b* genes within a unitary epigenetic domain targeted to *chkb* may be common to eutherians.

The apposition of the *chkb* and *cpt1b* genes occurred in mammals subsequent to the divergence of marsupials.

The activities of CHKB and CPT1B, rate-limiting for PC and acylcarnitine synthesis respectively, have the potential to mutually reinforce the capacity for mitochondrial FAO, which is supported by the outcomes of naturally occurring and induced mutations of these genes. Thus, it is possible that this regulatory linkage is an important component of lipid metabolism in mammals. In order to address this possibility, a phylogenetic approach was used to map the genomic arrangement of the *chkb* and *cpt1b* genes among extant animals with sequenced and annotated genomes that span vertebrate evolution. As shown in Figure 6a, the *chkb* and *cpt1b* genes are unlinked in lamprey (*Petromyzon marinus*) and a shark (*Callorhinchus milii*) and became distally syntenic prior to the divergence of bony fish, indicated by the 9.3 kb intergenic distance in zebrafish (*Danio rerio*) and coelacanth (*Latimeria chalumnae*). This distal synteny is conserved in amphibians (*e.g. Xenopus tropicalis*) but was lost in birds (*e.g. Gallus gallus*) and reptiles (*e.g. Anolis carolinensis*) [50, 51].

The intergenic distance is reduced in a marsupial (*Monodelphis domestica*) to 2.3 kb, and in the earliest diverging placental mammals, represented by extant Xenarthrans such as the armadillo *Dasypus novemcinctus*, the intergenic distance is about 1 kb. An average intergenic distance of about 500 bp between syntenic *chkb* and *cpt1b* genes appears to be highly conserved among eutherian mammals, suggestive of positive selection. Thus, the timing of this transition to a close intergenic distance coincides with the emergence of eutherian mammals. The *chkb-cpt1b* loci of two additional marsupials, a wallaby (*Notamacropus eugenii*) and Tasmanian devil (*Sarcophilus harrisii*), are similar to *Monodelphis*, supporting a marsupial/eutherian dichotomy with respect to the *chkb-cpt1b* locus [50, 51]. Considering that many of the physiological and allometric differences between marsupials and eutherians are connected to distinctions in basal metabolic rate and energy expenditure [59–62], a modification of lipid metabolism at this point in mammalian evolution due to a novel *chkb-cpt1b* linkage is potentially significant. Consistent with this prediction, the most phylogenetically ancient mammal in which canonical thermogenic BAT depots have been identified is the tenrec *Echinops telfairi*, a protoendothermic eutherian mammal that maintains elevated body temperatures during reproduction through transient BAT formation around reproductive organs [63]. Thus, as the *E. telfairi* genome contains ~700 bp *Chkb-Cpt1b* intergenic distance (Figure 6a), the emergence of BAT occurred relatively soon after the condensation of the *chkb-cpt1b* locus that coincides with the divergence of marsupials and eutherians.

Chkb-cpt1b synteny is constrained by functional *UCP1*.

In considering the evolutionary emergence of BAT, it's intriguing to note that the *UCP1* gene was also lost in in the common saurian ancestor of birds and reptiles [64] in conjunction

with the loss of *chkb-cpt1b* synteny in this clade (Figure 6a). While reptiles remain as ectothermic heterotherms, relying on environmental warming to increase body temperature, birds have taken a distinct evolutionary route to achieve an elevated capacity for endothermy based on UCP1-independent thermogenesis in hypertrophic skeletal muscle depots [64–66]. The coincident loss of both *chkb-cpt1b* synteny and the *UCP1* gene in this clade, in contrast to the conserved proximal *chkb-cpt1b* synteny in eutherians, supports a model in which the loss of the *UCP1* gene (and thus the potential for thermogenic proton leakage) eliminated the selective pressure to maintain conjoined *chkb* and *cpt1b* genes. In further support of this, despite the nearly complete loss of *chkb-cpt1b* synteny among saurians, *chkb-cpt1b* synteny with ~8 kb intergenic distance was retained in two distantly related members of this clade, the golden eagle (*Aquila chrysaetos canadensis*) and American alligator (*Alligator mississippiensis*) (Figure 6b) [50, 51]. This indicates that *UCP1* gene loss in the saurian ancestor preceded the loss of c*hkb-cpt1b* synteny, which then occurred independently in multiple lineages, suggesting that UCP1 function generates significant selective pressure to maintain *chkb-cpt1b* linkage.

As an additional assessment of the apparent correlation between functional UCP1 and *chkb-cpt1b* synteny, we compared the distribution of intergenic distance in UCP1-expressing eutherians with those that have lost UCP1 function (and thus the ability to develop BAT) due to genomic loss of the *UCP1* gene [67]. As shown in Figure 6c, the intergenic distance in $UCP1^{-}$ eutherians is significantly greater than in $UCP1^{+}$ eutherians, consistent with the relaxation of a constraint for tight *chkb-cpt1b* synteny resulting from the loss of UCP1 function in these lineages. These observations of a strong correlation between *chkb-cpt1b* apposition and UCP1 activity provide significant phylogenetic support for the causal relevance of conjoined *chkb* and *cpt1b* genes to the emergence of eutherian BAT.

Expression of the *chkb* and *cpt1b* genes is not coordinated in the marsupial *Monodelphis domestica*.

The working hypothesis that emerged from the presented findings is that the apposition of the *chkb* and *cpt1b* genes resulted in a functional transition from their independent expression to a coordinated mode of regulation due to the loss of functional intergenic sequences. This model predicts that the expression of *chkb* and *cpt1b* would be unlinked in species possessing a pre-eutherian locus structure, in contrast to what was observed in mice. Fortunately, the existence of an experimentally accessible marsupial provides a natural experiment to test this hypothesis, given the dichotomy of eutherian and marsupial *chkb-cpt1b* locus structure. The small laboratory opossum *Monodelphis domestica*, which possesses a 2.3 kb intergenic distance (Figure 1c, 6a), was employed to assess this prediction by surveying the tissue-specific expression of *chkb* and *cpt1b*. In contrast to the colocalization of *Chkb* and *Cpt1b* transcripts and the *Chkb-Cpt1b* fusion transcript observed in mice (Figure 2b), the expression of the *chkb* and *cpt1b* genes was unlinked in the marsupial, and the relative levels of expression of the genes among the tissues was different from that in mice with no fusion transcripts detected (Figure 7a). While both *chkb* and *cpt1b* were transcribed at high levels in opossum skeletal muscle, their mRNA levels in heart were low, in contrast to the more similar expression in these tissues in mice. The distribution of the opossum *cpt2* and *slc25a20* transcripts parallels the elevated expression of *cpt1b* in

skeletal muscle, consistent with their roles in the same fatty acid transport pathway. In addition, while both genes are expressed at low levels in mouse liver (Figure 2), *chkb* (but not *cpt1b*) is transcribed at a moderately high level in opossum liver. However, the most striking difference is the highest level of *chkb* transcripts (and concomitant low level of *cpt1b* mRNA) in opossum WAT, which contrasts with the low level of transcription of both genes in mouse WAT (Figure 2b). Collectively, these observations reinforce the possibility that the deletion of the *chkb-cpt1b* intergenic sequence precipitated the coordination of *chkb* and *cpt1b* expression in eutherians, such that the remaining intergenic sequence in opossum, albeit reduced in size from the ~9 kb span in fish and amphibians, is sufficient to maintain independent *chkb* and *cpt1b* expression likely through the action of specific retained *cis*-acting regulatory sequences in this region.

These observations also suggest that the opossum *chkb* gene is associated with a strong WAT-specific enhancer, which may have directed novel *cpt1b* expression in this compartment following the intergenic deletion that brought *cpt1b* closer to the *chkb* 5'-flanking region if it was functional in the MRCA. Notably, the intergenic sequence in *Monodelphis* contains a CGI that may contribute to the expression of marsupial *cpt1b* in skeletal muscle (and its suppression in WAT and liver) and is encompassed in the intergenic deletion in eutherians (Figure 1c). The loss of putative functional elements in this region may have facilitated the co-option of *cpt1b* regulation by *chkb* 5'-flanking sequences, leading to the novel co-expression of *chkb* and *cpt1b* in an adipocyte lineage in the eutherian ancestor that provided for the subsequent acquisition of the BAT phenotype, where both genes are highly expressed (Figure 2b). Furthermore, the high degree of apparent positive selection for *chkb-cpt1b* apposition among eutherian mammals (in light of the repeated loss of synteny in saurians) suggests that this event may have had significant implications for mammalian physiology and the emergence of placental mammals.

Independent domains of histone modification and RNA polymerase II initiation are targeted to the *chkb* and *cpt1b* genes in opossum.

The unlinked expression of the *chkb* and *cpt1b* genes in opossum, in contrast to the parallel tissue distribution of their expression in mice, raises the question of whether this disparity was also associated with a distinction in chromatin modification at the *chkb-cpt1b* locus that could reflect distinct mechanisms of gene regulation at the eutherian and marsupial loci. To address this, ChIP assays for acetyl-H3 were performed with chromatin prepared from opossum heart and skeletal muscle. The results showed a marked distinction from the patterns of H3 acetylation observed in mouse cells. In contrast to a single peak of histone acetylation localized to the 5' end of *Chkb* in mice (Figure 3), distinct peaks of H3 acetylation and were localized to the *chkb* gene (amplicons o3 and o4) and to the CGI located upstream of the *cpt1b* gene in opossum (amplicon o7) (Figure 7b,c). The distinct peak upstream of *cpt1b* displayed the highest level of H3 acetylation in the opossum locus and was absent in the mouse locus (Figure 3). Since this sequence was lost in the eutherian intergenic deletion it may have eliminated a putative enhancer or chromatin domain boundary function, or elements associated with the independent transcription of *cpt1b*, allowing the *chkb* 5'-flanking region to co-opt the transcriptional regulation of *cpt1b*. Concomitantly, this may have also allowed conserved functional sequences in the *cpt1b*

proximal 5'-flanking region, such as the FARE and other elements, to reciprocally affect the transcription of *chkb* as supported by the coordinated response of mouse *Chkb* and *Cpt1b* to palmitate (Figure 2c).

In order to further assess the potential for independent transcription of the opossum *cpt1b* gene, a ChIP assay for H3K4me3 was performed as a marker for sites of transcription initiation in opossum skeletal muscle where both genes are highly expressed (Figure 7). As was seen in mice (Figure 4a), a peak of H3K4me3 was localized at the 5' end of the opossum *chkb* gene (amplicon o3; Figure 8a). However, in contrast to the mouse locus, a second robust peak of H3K4me3 was also localized upstream of *cpt1b* at the CGI (amplicon o7). A ChIP assay for serine 5-phosphorylated RNAP in opossum skeletal muscle also showed a second domain of recruitment adjacent to the intergenic CGI island (amplicon o6; Figure 8b), consistent with intergenic transcription initiation. Concomitantly, a ChIP for serine 2-phosphorylated RNAPII revealed discrete domains of elongating RNAPII downstream of these sites of initiation (Figure 8c). Considered together, the patterns of H3 acetylation and methylation and RNAPII recruitment support the inference from the disparate tissue specific expression of *chkb* and *cpt1b* that these genes are independently transcribed in opossum. Significantly, the sites of intergenic histone modification and RNAPII initiation in the opossum locus are colocalized with the CGI, suggesting that specific sequences in this region are involved in the independent transcription of *cpt1b* that were lost in the eutherian locus. It should be noted that the precise 5' ends of opossum *cpt1b* transcripts have not been mapped, such that transcription initiation in the CGI region is possible. Our interpretation of these findings is that it is the loss of specific functional elements in the intergenic region, not the reduction in intergenic distance *per se*, that distinguishes the eutherian and marsupial *chkb-cpt1b* loci. However, as *cpt1b* then became dependent on the *chkb* promoter for transcription in this model, the short intergenic distance became functionally significant and selected for in eutherians.

A model for the emergence of BAT in a background of neutral UCP1 evolution.

In extant eutherians, the distinguishing phenotype of brown adipocytes includes the coincidence of multilocular lipid droplets, UCP1 expression, numerous mitochondria, and endogenous FAO. However, UCP1 has been under neutral selection since the emergence of bony fish, and a persistent paradox is the ability of marsupials to produce multilocular adipocytes that express functional UCP1 but cannot form thermogenic BAT. Indeed, the *ex vivo* induction of multilocular adipocytes from embryonic limb bud mesenchyme has been demonstrated in chicken [64], and cold-induced multilocular adipocytes have been shown in Muscovy ducks, but with few mitochondria compared to mammalian BAT [68]. These observations show that the underlying mechanism for inducing multilocular adipocytes, which increases the surface area for lipolysis, has been in place since before the emergence of mammals and suggest that the defining characteristic of eutherian BAT is thus an elevated capacity for FAO in these cells. We propose that the coordinated high levels of co-expression of *chkb* and *cpt1b* in a multilocular adipocyte lineage due to an intergenic deletion in the eutherian ancestor was a precipitating event that provided for the elevated mitochondrial FAO that caused these cells to become BAT, and may have thus contributed significantly to the evolution of eutherian mammals.

In this model (Figure 9), *chkb* and *cpt1b* were initially independently transcribed from discrete insulated regulatory domains in the therian ancestor, as is retained in marsupials. Upon deletion of the majority of intergenic sequence, a putative regulatory region associated with the intergenic CGI in opossum that maintained independent *cpt1b* expression was lost, and dominant regulation of *cpt1b* was subsequently co-opted by *chkb*-associated regulatory sequences (with potential reciprocal effects of *cpt1b*-associated elements on *chkb* transcription), which drove novel elevated *cpt1b* expression in adipocytes in parallel with extant *chkb* expression. The resulting increase in both mitochondrial fatty acid flux and PC synthesis for mitochondrial membrane biogenesis drove an increase in endogenous FAO, providing for thermogenic levels of proton flux and the emergence of the brown adipocyte phenotype. The co-expression of *chkb* and *cpt1b*, likely through independently functioning factor binding sites at each gene, may also be important for muscle FAO, and appears to have been in place prior to the marsupial/eutherian divergence, evidenced by their relatively high co-expression in opossum skeletal muscle (Figure 7a).

While the juxtaposition of the *cpt1b* gene to a putative strong WAT-specific enhancer (as appears to be associated with the opossum *chkb* gene) provides a potential molecular mechanism for the novel expression of *cpt1b* in an adipocyte lineage (and thus the capacity for endogenous FAO), this also raises the question of the role of elevated *chkb* expression observed in marsupial WAT (Figure 7). An intriguing possibility is that it is causally linked to the ability of marsupials to generate multilocular adipocytes in WAT, as is also characteristic of eutherian beige and brown adipocytes. Cytoplasmic lipid droplets are composed of a triglyceride core encapsulated by a phospholipid monolayer comprised predominantly of PC [69] such that the formation of multilocular droplets with greater total lipid droplet surface area may require elevated *de novo* PC synthesis, accounting for the high level of *chkb* expression in opossum WAT. This would provide for elevated lipolysis to generate secreted fatty acids for FAO in skeletal muscle, where *cpt1b* expression is high (Figure 7a). Thus, the primordial marsupial BAT may only be lacking the capacity for endogenous FAO provided by *cpt1b* expression to become thermogenic. *Chkb* expression was subsequently maintained at a high level in eutherian BAT upon the linkage of the *chkb* and *cpt1b* genes (Figure 2b), providing PC for both lipid droplet and mitochondrial membrane synthesis. The low expression levels of *Chkb* and *Cpt1b* in mouse WAT (in contrast to their highest expression in BAT) further suggests the maintenance of a distinct pathway in eutherians for the ontogeny of white adipocytes with a transcriptionally inactive *chkb-cpt1b* locus (Figure 2b), consistent with current models for the distinct developmental origins of white and brown preadipocytes [70].

Conclusions

The acquisition of BAT was a major evolutionary achievement in mammals that significantly affected the scope of mammalian physiology, life history, and geography. In addition, the FAO capacity of BAT has made it a potential therapeutic target to counteract a positive lipid balance in the treatment of obesity. The central role of UCP1 in BAT function has been firmly established, both biochemically and genetically, but the mechanistic basis for the emergence of BAT in eutherian mammals has remained elusive. While previous studies have characterized the functional evolution of the UCP gene family, they have also revealed the

insufficiency of UCP1 evolution alone to account for BAT function, and led to the prediction that the acquisition of elevated mitochondrial oxidative capacity likely played a predominant role [40]. Consistent with this prediction, we conclude from the findings presented here that the convergence of the *chkb* and *cpt1b* genes in a common transcriptional regulatory domain in the eutherian ancestor resulted in their coordinated expression, and provided for the novel attainment of elevated mitochondrial FAO in an extant multilocular adipocyte lineage that became canonical thermogenic BAT as a direct result of this event. Ongoing studies will resolve the molecular mechanisms of the transcriptional and epigenetic co-regulation of the *chkb* and *cpt1b* genes, and the significance of their co-expression to mitochondrial structure, cellular FAO capacity, and thermogenesis in eutherian striated muscle and BAT to test this hypothesis.

Materials and Methods

Cell culture.

Mouse C2C12 myoblast cells (ATCC, Manassas, VA), DE2.3 brown preadipocyte cells [71] (a gift of Bruce Spiegelman, Harvard University), and primary female human myoblasts (a gift of Joseph Houmard, East Carolina University) were maintained in Dulbecco's modified Eagle's medium (DMEM, Mediatech, Manassas, VA) supplemented with 10% fetal bovine serum (Gemini Bio Products, West Sacramento, CA), 100 U/ml penicillin, 100 μg/ml streptomycin, and 250 ng/ml amphotericin B (Gibco, Gaithersburg, MD). Upon reaching 80–90% confluency, differentiation was induced by replacing growth medium with low-serum DMEM containing 1% FBS, 100 U/ml penicillin, 100 μg/ml streptomycin, and 250 ng/ml amphotericin B. On day six of differentiation verified microscopically by the formation of syncytial myotubes and multilocular lipid droplets, respectively, myotubes and brown adipocytes were harvested for analysis. To prepare BSA-conjugated palmitate, a solution of 1.7 mM fatty acid free BSA (Sigma-Aldrich, St. Louis, MO) and 750 mM NaCl was prepared. Separately, 61.2 mg of sodium palmitate (TCI America, Portland, OR) was dissolved in 17.6 ml of 750 mM NaCl at 70°C with stirring until clear. To make BSA-conjugated 5 mM palmitate, the palmitate solution was mixed with 20 ml of pre-warmed BSA solution at 37°C with stirring until clear, then diluted 1:2 with 750mM NaCl. A control solution containing only BSA was prepared in parallel. Solutions were adjusted pH 7.4 with 1N NaOH, sterile filtered, and stored −20° C. For the palmitate treatment experiment, cells were washed with PBS and treted with fresh media containing 50 μM BSA-palmitate or BSA vehicle control for 4 h prior to transcript analysis.

Mouse and opossum tissue harvest and primary cell culture.

Tissues from female C57BL/6 mice (a gift of Kym Gowdy, East Carolina University) were snap frozen in liquid nitrogen and stored at −80° C until analysis of mRNA and chromatin. Cultures of primary mouse myotubes were prepared as previously described [72, 73]. In short, freshly harvested gastrocnemius muscle was digested in 0.05% trypsin with 0.53 mM EDTA and cultured in DMEM containing 4.5 g/L glucose, 10% FBS, 100 U/ml penicillin, 100 μg/ml streptomycin, and 250 ng/ml amphotericin B. After repeated selective passage to remove fibroblasts, enriched myoblasts were differentiated in DMEM containing 1.0 g/L glucose, 1% FBS, 100 U/ml penicillin, 100 μg/ml streptomycin, and 250 ng/ml amphotericin

B. Cultures of primary mouse brown preadipocytes were prepared as previously described [74]. Briefly, intrascapular brown adipose tissue was digested in 1.5 mg/ml collagenase A and cultured in the same growth medium as primary skeletal muscle cells. Differentiation was induced with DMEM containing 4.5 g/L glucose, 10% FBS, 0.5 μM IBMX, 5 μM dexamethasone, 20 nM insulin,1 nM T3 , 125 μM indomethacin (each from Sigma-Aldrich, St. Louis, MO), 100 U/ml penicillin, 100 μg/ml streptomycin, and 250 ng/ml amphotericin B. The Sears Lab (UCLA) maintains a breeding colony of opossums (*Monodelphis domestica*) using established protocols [75, 76]. This colony is comprised of pedigreed animals from the Texas Biomedical Research Institute (San Antonio, TX) and their descendants. Adult female opossums were euthanized by carbon dioxide inhalation to effect followed by cervical dislocation, and appropriate tissues dissected. All procedures have been approved by the ECU and UCLA IACUC.

mRNA purification and qRT-PCR.

All primers for quantitative reverse transcription and PCR (qRT-PCR; Table 1) and genomic quantitative PCR (qPCR; Table 2) were designed and validated as previously described to ensure that the requirements for quantification by the comparative threshold cycle (C_t) method were met [77]. RNA purification, cDNA synthesis, and qPCR were performed as previously validated and described in detail [77]. Briefly, frozen tissue was finely ground in liquid nitrogen and RNA was purified with Trizol reagent according to the manufacturer's instructions, and reverse transcribed using the Verso cDNA synthesis kit (Thermo Fisher Scientific, Waltham, MA). QPCR was performed with Power SYBR Green PCR Master Mix (Thermo Fisher Scientific) in accordance with manufacturer's instructions using a C1000 Touch™ Thermal Cycler (Bio-Rad, Hercules, CA). The specified primer pairs are shown in Table 1. Transcript levels were measured by the comparative C_t method using beta-2 microglobulin (B2M) as an internal control.

Chromatin immunoprecipitation assay (CHIP).

ChIP assays and analysis of fractions by qPCR were performed as previously validated and described in detail [77]. Primer sequences are shown in Table 2. Frozen tissue samples were finely ground in liquid nitrogen prior to the fixation and lysis procedure. Antibodies against the following epitopes were used: normal rabbit IgG control (Millipore, Burlington, MA, #12–370), panacetyl-H3 (Millipore #06599MI), trimethyl-H3Lys4 (Millipore #0473MI), RNA polymerase II CTD repeat (phospho-Ser5, Abcam, Cambridge, MA, #ab5131), RNA polymerase II CTD repeat (phospho-Ser2, Abcam #ab5095) and PRDM16 (Sigma Aldrich #SAB3500989). Bound:input ratios were determined by the comparative C_t value method as Bound/Input=$2^{(\text{input Ct-bound Ct})}$ using a 1% v/v aliquot of input chromatin.

Western blot of CPT1B.

Finely ground frozen tissue was used to prepare whole cell lysates for resolution by SDS-PAGE, transfer to PVDF membrane, and immunodetection as previously described in detail [78]. The anti-CPT1B rabbit polyclonal antibody (Thermo Fisher Scientific #PA5–79065) was used at a 1:500 dilution. Beta tubulin was detected as a loading control using a previously described monoclonal antibody [78].

Phylogenetic analysis of *chkb-cpt1b* loci.

The intergenic distances between *chkb* and *cpt1b* genes in the indicated species were determined using the publicly available Genome Browser [50] at the University of California Santa Cruz Genomics Institute (http://genome.ucsc.edu) and the associated annotation tracks [51]. *Chkb-cpt1b* intergenic distances were calculated from the endpoints of the most proximate mapped reference transcripts for the genes. In species for which the *chkb* and *cpt1b* transcripts have not been directly mapped, the endpoints of the alignments with the orthologous mouse transcripts was used, which was corroborated by gene prediction algorithms. The set of $UCP1^{+}$ eutherians analyzed in Figure 6c consists of human (*Homo sapiens)*, tarsier (*Tarsus syrichta*), tree shrew (*Tupaia belangeri*), mouse (*Mus musculus*), squirrel (*Spermophilius tridecemlineatus*), pika (*Ochotona princeps*), cat (*Felis catus*), dog (*Canis lupus*), microbat (*Myotis lucifugus*), and tenrec (*Echinops telfairi*). The set of $UCP1^{-}$ eutherians consists of pig (*Sus scrofa*), rock hyrax (*Procavia capensis*), elephant (*Loxodonta africana*), horse (*Equus caballus*), cow (*Bos taurus*), dolphin (*Tursiops truncatus*), minke whale (*Balaenoptera acutorostrata scammoni*), manatee *(Trichechus manatus latirostris*), Chinese pangolin (*Manis pentadactyla*), and armadillo (*Dasypus novemcinctus*) [67].

Statistical analysis.

Statistical significance of observed differences was determined by ANOVA and a *post hoc* Tukey-Kramer multiple comparison test to identify highly significant differences (α=0.05).

Acknowledgements

The opossum colony at UCLA is supported by a grant from the National Institutes of Health (R21 OD022988 to K.E.S.).

Abbreviations

ATP	adenosine triphosphate
FAO	fatty acid oxidation
NADH	nicotinamide adenine dinucleotide
$FADH_2$	flavin adenine dinucleotide
CoA	coenzyme A
TCA	tricarboxylic acid
PC	phosphatidylcholine
BAT	brown adipose tissue
WAT	white adipose tissue
MRCA	most recent common ancestor

References

[1]. McGarry JD, Brown NF. The mitochondrial carnitine palmitoyltransferase system. From concept to molecular analysis. Eur J Biochem. 1997;244:1–14. [PubMed: 9063439]

[2]. Brandt JM, Djouadi F, Kelly DP. Fatty acids activate transcription of the muscle carnitine palmitoyltransferase I gene in cardiac myocytes via the peroxisome proliferator-activated receptor alpha. J Biol Chem. 1998;273:23786–92. [PubMed: 9726988]

[3]. Chamouton J, Latruffe N. PPARalpha/HNF4alpha interplay on diversified responsive elements. Relevance in the regulation of liver peroxisomal fatty acid catabolism. Curr Drug Metab. 2012;13:1436–53. [PubMed: 22978398]

[4]. Gilde AJ, van der Lee KA, Willemsen PH, Chinetti G, van der Leij FR, van der Vusse GJ, et al. Peroxisome proliferator-activated receptor (PPAR) alpha and PPARbeta/delta, but not PPARgamma, modulate the expression of genes involved in cardiac lipid metabolism. Circ Res. 2003;92:518–24. [PubMed: 12600885]

[5]. Martinez-Jimenez CP, Kyrmizi I, Cardot P, Gonzalez FJ, Talianidis I. Hepatocyte nuclear factor 4alpha coordinates a transcription factor network regulating hepatic fatty acid metabolism. Mol Cell Biol. 2010;30:565–77. [PubMed: 19933841]

[6]. Muoio DM, MacLean PS, Lang DB, Li S, Houmard JA, Way JM, et al. Fatty acid homeostasis and induction of lipid regulatory genes in skeletal muscles of peroxisome proliferator-activated receptor (PPAR) alpha knock-out mice. Evidence for compensatory regulation by PPAR delta. J Biol Chem. 2002;277:26089–97. [PubMed: 12118038]

[7]. Yu GS, Lu YC, Gulick T. Co-regulation of tissue-specific alternative human carnitine palmitoyltransferase Ibeta gene promoters by fatty acid enzyme substrate. J Biol Chem. 1998;273:32901–9. [PubMed: 9830040]

[8]. Moore ML, Park EA, McMillin JB. Upstream stimulatory factor represses the induction of carnitine palmitoyltransferase-Ibeta expression by PGC-1. J Biol Chem. 2003;278:17263–8. [PubMed: 12611894]

[9]. Sharma V, Dhillon P, Parsons H, Allard MF, McNeill JH. Metoprolol represses PGC1alpha-mediated carnitine palmitoyltransferase-1B expression in the diabetic heart. Eur J Pharmacol. 2009;607:156–66. [PubMed: 19233164]

[10]. Maples JM, Brault JJ, Witczak CA, Park S, Hubal MJ, Weber TM, et al. Differential epigenetic and transcriptional response of the skeletal muscle carnitine palmitoyltransferase 1B (CPT1B) gene to lipid exposure with obesity. Am J Physiol Endocrinol Metab. 2015;309:E345–56. [PubMed: 26058865]

[11]. Baldan A, Relat J, Marrero PF, Haro D. Functional interaction between peroxisome proliferator-activated receptors-alpha and Mef-2C on human carnitine palmitoyltransferase 1beta (CPT1beta) gene activation. Nucleic Acids Res. 2004;32:4742–9. [PubMed: 15356291]

[12]. Yuan H, Niu Y, Liu X, Fu L. Exercise increases the binding of MEF2A to the Cpt1b promoter in mouse skeletal muscle. Acta Physiol (Oxf). 2014;212:283–92. [PubMed: 25213552]

[13]. van der Leij FR, Cox KB, Jackson VN, Huijkman NCA, Bartelds B, Kuipers JRG, et al. Structural and Functional Genomics of the CPT1B Gene for Muscle-type Carnitine Palmitoyltransferase I in Mammals. Journal of Biological Chemistry. 2002;277:26994–7005.

[14]. Moore ML, Wang GL, Belaguli NS, Schwartz RJ, McMillin JB. GATA-4 and serum response factor regulate transcription of the muscle-specific carnitine palmitoyltransferase I beta in rat heart. J Biol Chem. 2001;276:1026–33. [PubMed: 11038368]

[15]. Wu G, Vance DE. Choline kinase and its function. Biochem Cell Biol. 2010;88:559–64. [PubMed: 20651826]

[16]. Yamazaki N, Yamanaka Y, Hashimoto Y, Hiramatsu T, Shinohara Y, Terada H. The gene encoding muscle-type carnitine palmitoyltransferase I: comparison of the 5'-upstream region of human and rodent genes. J Biochem. 2003;133:523–32. [PubMed: 12761301]

[17]. Yamazaki N, Shinohara Y, Kajimoto K, Shindo M, Terada H. Novel expression of equivocal messages containing both regions of choline/ethanolamine kinase and muscle type carnitine palmitoyltransferase I. J Biol Chem. 2000;275:31739–46. [PubMed: 10918069]

[18]. Kuan CS, Yee YH, See Too WC, Few LL. Ets and GATA transcription factors play a critical role in PMA-mediated repression of the ckbeta promoter via the protein kinase C signaling pathway. PLoS One. 2014;9:e113485. [PubMed: 25490397]

[19]. Ji S, You Y, Kerner J, Hoppel CL, Schoeb TR, Chick WS, et al. Homozygous carnitine palmitoyltransferase 1b (muscle isoform) deficiency is lethal in the mouse. Mol Genet Metab. 2008;93:314–22. [PubMed: 18023382]

[20]. Auinger A, Rubin D, Sabandal M, Helwig U, Ruther A, Schreiber S, et al. A common haplotype of carnitine palmitoyltransferase 1b is associated with the metabolic syndrome. Br J Nutr. 2013;109:810–5. [PubMed: 22809552]

[21]. Maples JM, Brault JJ, Shewchuk BM, Witczak CA, Zou K, Rowland N, et al. Lipid exposure elicits differential responses in gene expression and DNA methylation in primary human skeletal muscle cells from severely obese women. Physiol Genomics. 2015;47:139–46. [PubMed: 25670728]

[22]. Bruce CR, Hoy AJ, Turner N, Watt MJ, Allen TL, Carpenter K, et al. Overexpression of carnitine palmitoyltransferase-1 in skeletal muscle is sufficient to enhance fatty acid oxidation and improve high-fat diet-induced insulin resistance. Diabetes. 2009;58:550–8. [PubMed: 19073774]

[23]. Koves TR, Ussher JR, Noland RC, Slentz D, Mosedale M, Ilkayeva O, et al. Mitochondrial overload and incomplete fatty acid oxidation contribute to skeletal muscle insulin resistance. Cell Metab. 2008;7:45–56. [PubMed: 18177724]

[24]. Cohen P, Spiegelman BM. Cell biology of fat storage. Mol Biol Cell. 2016;27:2523–7. [PubMed: 27528697]

[25]. Cohen P, Spiegelman BM. Brown and Beige Fat: Molecular Parts of a Thermogenic Machine. Diabetes. 2015;64:2346–51. [PubMed: 26050670]

[26]. Oelkrug R, Polymeropoulos ET, Jastroch M. Brown adipose tissue: physiological function and evolutionary significance. J Comp Physiol B. 2015;185:587–606. [PubMed: 25966796]

[27]. Cedikova M, Kripnerova M, Dvorakova J, Pitule P, Grundmanova M, Babuska V, et al. Mitochondria in White, Brown, and Beige Adipocytes. Stem Cells Int. 2016;2016:6067349. [PubMed: 27073398]

[28]. Fuller-Jackson JP, Henry BA. Adipose and skeletal muscle thermogenesis: studies from large animals. J Endocrinol. 2018;237:R99–R115. [PubMed: 29703782]

[29]. Periasamy M, Herrera JL, Reis FCG. Skeletal Muscle Thermogenesis and Its Role in Whole Body Energy Metabolism. Diabetes Metab J. 2017;41:327–36. [PubMed: 29086530]

[30]. Nowack J, Giroud S, Arnold W, Ruf T. Muscle Non-shivering Thermogenesis and Its Role in the Evolution of Endothermy. Frontiers in Physiology. 2017;8.

[31]. Bal NC, Singh S, Reis FCG, Maurya SK, Pani S, Rowland LA, et al. Both brown adipose tissue and skeletal muscle thermogenesis processes are activated during mild to severe cold adaptation in mice. J Biol Chem. 2017;292:16616–25. [PubMed: 28794154]

[32]. Wu J, Bostrom P, Sparks LM, Ye L, Choi JH, Giang AH, et al. Beige adipocytes are a distinct type of thermogenic fat cell in mouse and human. Cell. 2012;150:366–76. [PubMed: 22796012]

[33]. Seale P, Conroe HM, Estall J, Kajimura S, Frontini A, Ishibashi J, et al. Prdm16 determines the thermogenic program of subcutaneous white adipose tissue in mice. J Clin Invest. 2011;121:96–105. [PubMed: 21123942]

[34]. Jastroch M, Wuertz S, Kloas W, Klingenspor M. Uncoupling protein 1 in fish uncovers an ancient evolutionary history of mammalian nonshivering thermogenesis. Physiol Genomics. 2005;22:150–6. [PubMed: 15886331]

[35]. Jastroch M, Buckingham JA, Helwig M, Klingenspor M, Brand MD. Functional characterisation of UCP1 in the common carp: uncoupling activity in liver mitochondria and cold-induced expression in the brain. J Comp Physiol B. 2007;177:743–52. [PubMed: 17576568]

[36]. Mzilikazi N, Jastroch M, Meyer CW, Klingenspor M. The molecular and biochemical basis of nonshivering thermogenesis in an African endemic mammal, Elephantulus myurus. Am J Physiol Regul Integr Comp Physiol. 2007;293:R2120–7. [PubMed: 17686883]

[37]. Jastroch M, Withers KW, Taudien S, Frappell PB, Helwig M, Fromme T, et al. Marsupial uncoupling protein 1 sheds light on the evolution of mammalian nonshivering thermogenesis. Physiol Genomics. 2008;32:161–9. [PubMed: 17971503]

[38]. Jastroch M, Withers KW, Stoehr S, Klingenspor M. Mitochondrial proton conductance in skeletal muscle of a cold-exposed marsupial, Antechinus flavipes, is unlikely to be involved in adaptive nonshivering thermogenesis but displays increased sensitivity toward carbon-centered radicals. Physiol Biochem Zool. 2009;82:447–54. [PubMed: 19614545]

[39]. Klingenspor M, Fromme T, Hughes DA Jr., Manzke L, Polymeropoulos E, Riemann T, et al. An ancient look at UCP1. Biochim Biophys Acta. 2008;1777:637–41. [PubMed: 18396149]

[40]. Hughes DA, Jastroch M, Stoneking M, Klingenspor M. Molecular evolution of UCP1 and the evolutionary history of mammalian non-shivering thermogenesis. BMC Evol Biol. 2009;9:4. [PubMed: 19128480]

[41]. Jastroch M, Oelkrug R, Keipert S. Insights into brown adipose tissue evolution and function from non-model organisms. J Exp Biol. 2018;221.

[42]. Sher RB, Aoyama C, Huebsch KA, Ji S, Kerner J, Yang Y, et al. A rostrocaudal muscular dystrophy caused by a defect in choline kinase beta, the first enzyme in phosphatidylcholine biosynthesis. J Biol Chem. 2006;281:4938–48. [PubMed: 16371353]

[43]. Wu G, Sher RB, Cox GA, Vance DE. Understanding the muscular dystrophy caused by deletion of choline kinase beta in mice. Biochim Biophys Acta. 2009;1791:347–56. [PubMed: 19236939]

[44]. Mitsuhashi S, Hatakeyama H, Karahashi M, Koumura T, Nonaka I, Hayashi YK, et al. Muscle choline kinase beta defect causes mitochondrial dysfunction and increased mitophagy. Hum Mol Genet. 2011;20:3841–51. [PubMed: 21750112]

[45]. Mitsuhashi S, Ohkuma A, Talim B, Karahashi M, Koumura T, Aoyama C, et al. A congenital muscular dystrophy with mitochondrial structural abnormalities caused by defective de novo phosphatidylcholine biosynthesis. Am J Hum Genet. 2011;88:845–51. [PubMed: 21665002]

[46]. Gutierrez Rios P, Kalra AA, Wilson JD, Tanji K, Akman HO, Area Gomez E, et al. Congenital megaconial myopathy due to a novel defect in the choline kinase Beta gene. Arch Neurol. 2012;69:657–61. [PubMed: 22782513]

[47]. Quinlivan R, Mitsuahashi S, Sewry C, Cirak S, Aoyama C, Mooore D, et al. Muscular dystrophy with large mitochondria associated with mutations in the CHKB gene in three British patients: extending the clinical and pathological phenotype. Neuromuscul Disord. 2013;23:549–56. [PubMed: 23692895]

[48]. Castro-Gago M, Dacruz-Alvarez D, Pintos-Martinez E, Beiras-Iglesias A, Delmiro A, Arenas J, et al. Exome sequencing identifies a CHKB mutation in Spanish patient with megaconial congenital muscular dystrophy and mtDNA depletion. Eur J Paediatr Neurol. 2014;18:796–800. [PubMed: 24997086]

[49]. Mitsuhashi S, Nishino I. Phospholipid synthetic defect and mitophagy in muscle disease. Autophagy. 2014;7:1559–61.

[50]. Kent WJ, Sugnet CW, Furey TS, Roskin KM, Pringle TH, Zahler AM, et al. The human genome browser at UCSC. Genome Res. 2002;12:996–1006. [PubMed: 12045153]

[51]. Raney BJ, Dreszer TR, Barber GP, Clawson H, Fujita PA, Wang T, et al. Track data hubs enable visualization of user-defined genome-wide annotations on the UCSC Genome Browser. Bioinformatics. 2014;30:1003–5. [PubMed: 24227676]

[52]. Prakash T, Sharma VK, Adati N, Ozawa R, Kumar N, Nishida Y, et al. Expression of conjoined genes: another mechanism for gene regulation in eukaryotes. PLoS One. 2010;5:e13284. [PubMed: 20967262]

[53]. Kim DS, Kim DW, Kim MY, Nam SH, Choi SH, Kim RN, et al. CACG: a database for comparative analysis of conjoined genes. Genomics. 2012;100:14–7. [PubMed: 22584068]

[54]. Kim RN, Kim A, Choi SH, Kim DS, Nam SH, Kim DW, et al. Novel mechanism of conjoined gene formation in the human genome. Funct Integr Genomics. 2012;12:45–61. [PubMed: 22231539]

[55]. Berger SL, Kouzarides T, Shiekhattar R, Shilatifard A. An operational definition of epigenetics. Genes Dev. 2009;23:781–3. [PubMed: 19339683]

[56]. Kimura H Histone modifications for human epigenome analysis. J Hum Genet. 2013;58:439–45. [PubMed: 23739122]

[57]. Harms MJ, Ishibashi J, Wang W, Lim HW, Goyama S, Sato T, et al. Prdm16 is required for the maintenance of brown adipocyte identity and function in adult mice. Cell Metab. 2014;19:593–604. [PubMed: 24703692]

[58]. Seale P, Bjork B, Yang W, Kajimura S, Chin S, Kuang S, et al. PRDM16 controls a brown fat/skeletal muscle switch. Nature. 2008;454:961–7. [PubMed: 18719582]

[59]. Lee AK, Cockburn A. Evolutionary ecology of marsupials Cambridge Cambridgeshire ; New York: Cambridge University Press; 1985.

[60]. McNab BK. Extreme measures : the ecological energetics of birds and mammals. Chicago: The University of Chicago Press; 2012.

[61]. McNab BK. Behavioral and ecological factors account for variation in the mass-independent energy expenditures of endotherms. J Comp Physiol B. 2015;185:1–13. [PubMed: 25155184]

[62]. McNab BK. An analysis of the factors that influence the level and scaling of mammalian BMR. Comp Biochem Physiol A Mol Integr Physiol. 2008;151:5–28. [PubMed: 18617429]

[63]. Oelkrug R, Goetze N, Exner C, Lee Y, Ganjam GK, Kutschke M, et al. Brown fat in a protoendothermic mammal fuels eutherian evolution. Nat Commun. 2013;4:2140. [PubMed: 23860571]

[64]. Mezentseva NV, Kumaratilake JS, Newman SA. The brown adipocyte differentiation pathway in birds: an evolutionary road not taken. BMC Biol. 2008;6:17. [PubMed: 18426587]

[65]. Newman SA. Thermogenesis, muscle hyperplasia, and the origin of birds. Bioessays. 2011;33:653–6. [PubMed: 21695679]

[66]. Newman SA, Mezentseva NV, Badyaev AV. Gene loss, thermogenesis, and the origin of birds. Ann N Y Acad Sci. 2013;1289:36–47. [PubMed: 23550607]

[67]. Gaudry MJ, Jastroch M, Treberg JR, Hofreiter M, Paijmans JLA, Starrett J, et al. Inactivation of thermogenic UCP1 as a historical contingency in multiple placental mammal clades. Science Advances. 2017;3:e1602878. [PubMed: 28706989]

[68]. Barre H, Cohen-Adad F, Duchamp C, Rouanet JL. Multilocular adipocytes from muscovy ducklings differentiated in response to cold acclimation. J Physiol. 1986;375:27–38. [PubMed: 3795059]

[69]. Bartz R, Li WH, Venables B, Zehmer JK, Roth MR, Welti R, et al. Lipidomics reveals that adiposomes store ether lipids and mediate phospholipid traffic. J Lipid Res. 2007;48:837–47. [PubMed: 17210984]

[70]. Kajimura S, Spiegelman BM, Seale P. Brown and Beige Fat: Physiological Roles beyond Heat Generation. Cell Metab. 2015;22:546–59. [PubMed: 26445512]

[71]. Pan D, Fujimoto M, Lopes A, Wang YX. Twist-1 is a PPARdelta-inducible, negative-feedback regulator of PGC-1alpha in brown fat metabolism. Cell. 2009;137:73–86. [PubMed: 19345188]

[72]. Hindi L, McMillan JD, Afroze D, Hindi SM, Kumar A. Isolation, Culturing, and Differentiation of Primary Myoblasts from Skeletal Muscle of Adult Mice. Bio Protoc. 2017;7.

[73]. Shahini A, Vydiam K, Choudhury D, Rajabian N, Nguyen T, Lei P, et al. Efficient and high yield isolation of myoblasts from skeletal muscle. Stem Cell Res. 2018;30:122–9. [PubMed: 29879622]

[74]. Klein J, Fasshauer M, Ito M, Lowell BB, Benito M, Kahn CR. beta(3)-adrenergic stimulation differentially inhibits insulin signaling and decreases insulin-induced glucose uptake in brown adipocytes. J Biol Chem. 1999;274:34795–802. [PubMed: 10574950]

[75]. Keyte AL, Smith KK. Basic Maintenance and Breeding of the Opossum Monodelphis domestica. CSH Protoc. 2008;2008:pdb prot5073.

[76]. Rousmaniere H, Silverman R, White RA, Sasaki MM, Wilson SD, Morrison JT, et al. Husbandry of Monodelphis domestica in the study of mammalian embryogenesis. Lab Anim (NY). 2010;39:219–26. [PubMed: 20567232]

[77]. Hogan KA, Jefferson HS, Karschner VA, Shewchuk BM. Expression of Pit-1 in nonsomatotrope cell lines induces human growth hormone locus control region histone modification and hGH-N transcription. J Mol Biol. 2009;390:26–44. [PubMed: 19427323]

[78]. Nakonechnaya AO, Jefferson HS, Chen X, Shewchuk BM. Differential effects of exogenous and autocrine growth hormone on LNCaP prostate cancer cell proliferation and survival. J Cell Biochem. 2013;114:1322–35. [PubMed: 23238889]

[79]. Kumar S, Hedges SB. A molecular timescale for vertebrate evolution. Nature. 1998;392:917–20. [PubMed: 9582070]

Research Highlights

- BAT thermogenesis is fueled by CPT1B-dependent fatty acid oxidation
- The *CPT1B* gene is conjoined to the *CHKB* gene exclusively in eutherians
- *CHKB-CPT1B* is transcribed within a unitary epigenetic domain in eutherians
- These genes are independently expressed from discrete domains in opossum
- *CHKB-CPT1B* conjoinment precipitated the emergence of BAT in eutherians

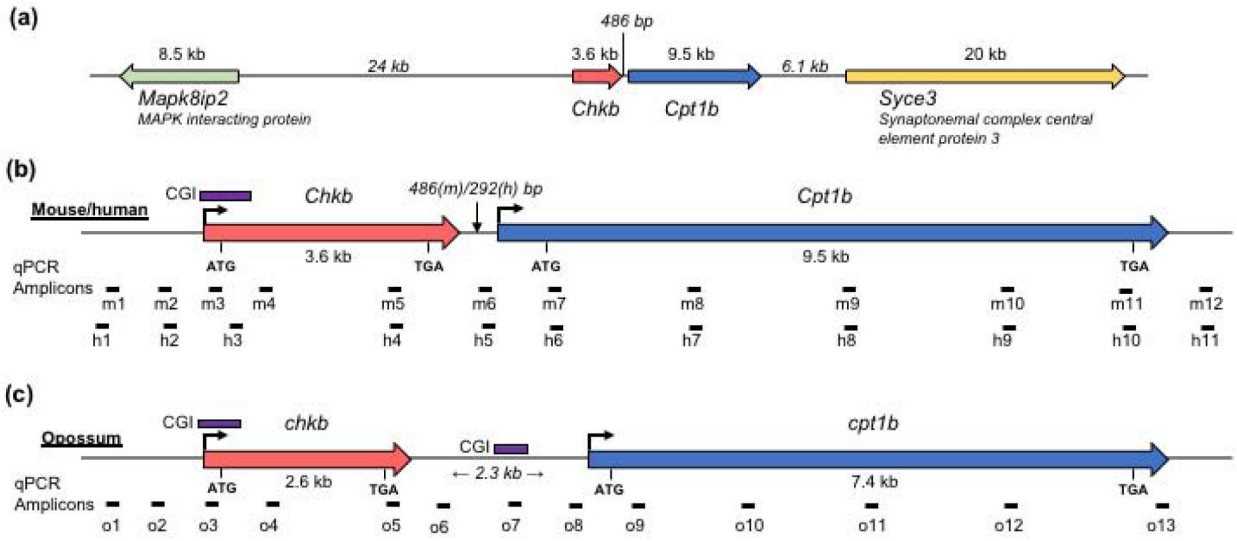

Figure 1. Structure of the *CHKB-CPT1B* locus.

(a) Map of ~75 kb of mouse chromosome 15qE3 containing the *Chkb* and *Cpt1b* genes, indicated by arrows showing transcriptional orientation. (b) Map of the mouse and human *CHKB-CPT1B* locus. (c) map of the opossum *chkb-cpt1b* locus. Transcription start sites are indicated by bent arrows. Locations of start and stop codons are indicated below the map. CpG islands (CGI) are delimited by purple bars above the map. The locations of ChIP assay amplicons are indicated below the maps.

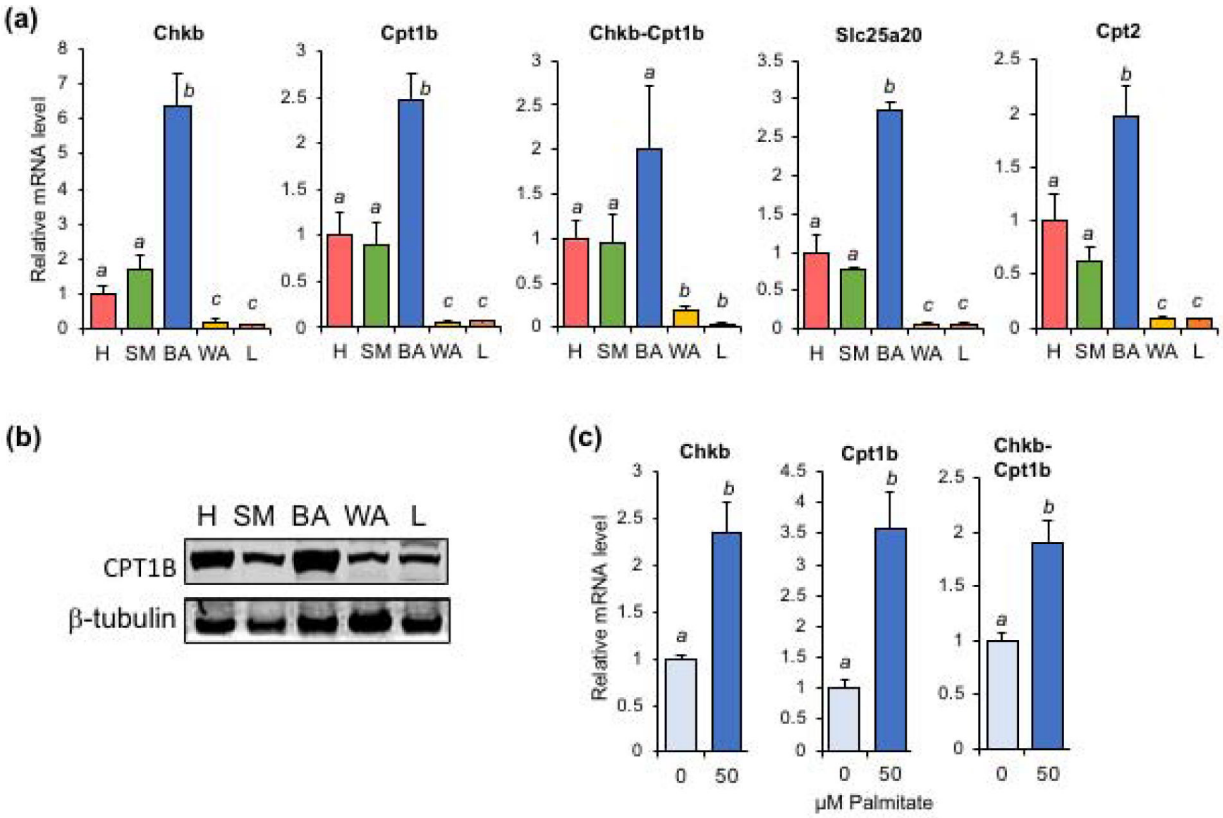

Figure 2. *Chkb* and *Cpt1b* expression are linked in mouse tissues and cell lines.

(a) *Chkb* and *Cpt1b* are differentially expressed in concert in mouse tissues: heart (H), skeletal muscle (SM), brown adipose tissue (BA), white adipose tissue (WA), liver (L). Internally controlled mRNA levels (vs. *β2-microglobulin* mRNA) were normalized to the level in heart. The data indicate the mean ± *SE* (*n*=3). ANOVA indicated significant differences among the tissues (P<0.001). Levels not connected by the same letter are significantly different as determined by a Tukey-Kramer multiple comparison test (P<0.05). (b) Immunoblot of CPT1B protein levels mirrors the relative transcript levels. (c) *Chkb, Cpt1b* and *Chkb-Cpt1b* fusion transcript levels are modulated in concert by palmitate. The data indicate the mean ± *SE* (*n*=3).

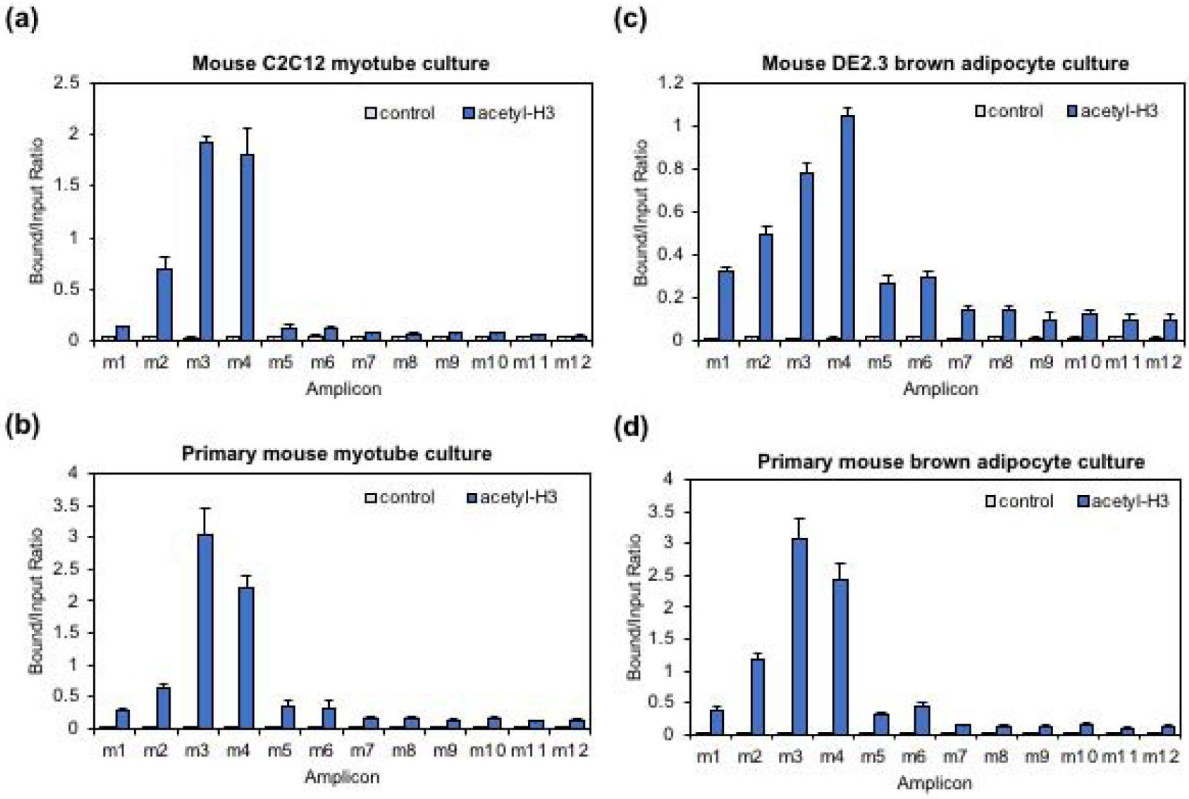

Figure 3. Elevated H3 acetylation is focused near the *CHKB* transcription start site in mice.

Results of ChIP assays with a panacetyl-H3 antibody. ChIP assay enrichment levels determined by qPCR, normalized to 1% v/v of input chromatin. The exponential qPCR data (C_t values) was antilog transformed to a linear expression of bound/input ratios as Bound/Input=$2^{(\text{input Ct-bound Ct})}$. (a) Mouse C2C12 myotubes. (b) Primary mouse myotubes. (c) Mouse DE2.3 brown adipocytes. (d) Primary mouse brown adipocytes. Amplicons are mapped in Figure 1b.

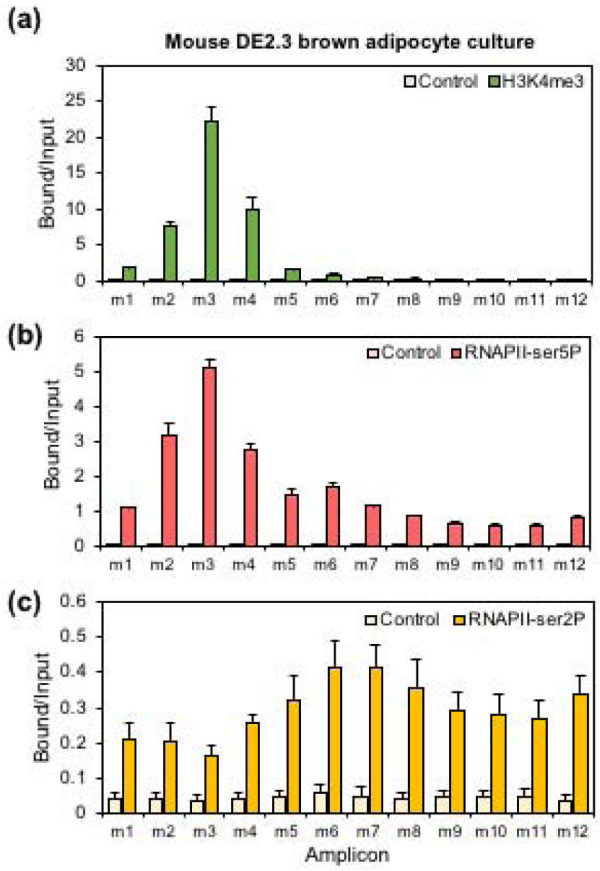

Figure 4. H3 lysine 4 trimethylation and RNAPII initiation are focused near the *CHKB* transcription start site in mouse DE2.3 brown adipocytes.

Results of ChIP assays. (a) H3 lysine 4 trimethylation. (b) RNAPII serine 5 phosphorylation (initiating form). (c) RNAPII serine 2 phosphorylation (elongating form). Amplicons are mapped in Figure 1b.

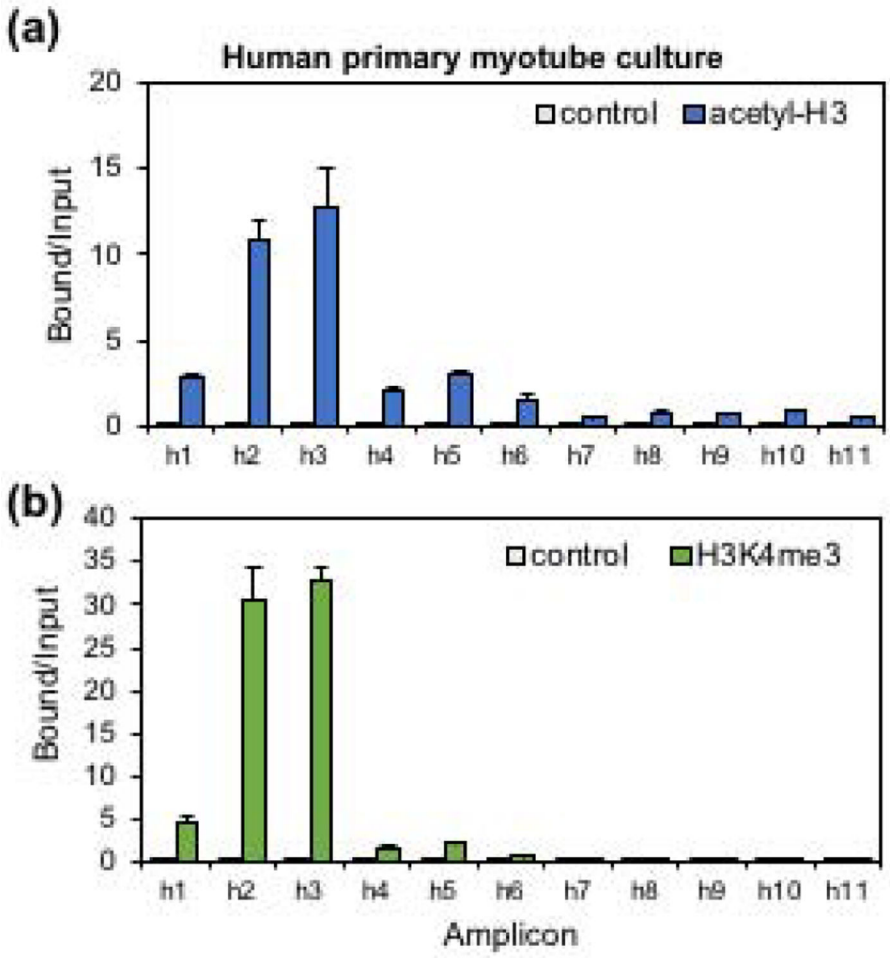

Figure 5. A single peak of histone modification is localized to the 5' end of the human *CHKB* gene in primary skeletal muscle myotubes.

Results of ChIP assays for (a) H3 acetylation and (b) H3 lysine 4 trimethylation. Amplicons are mapped in Figure 1b.

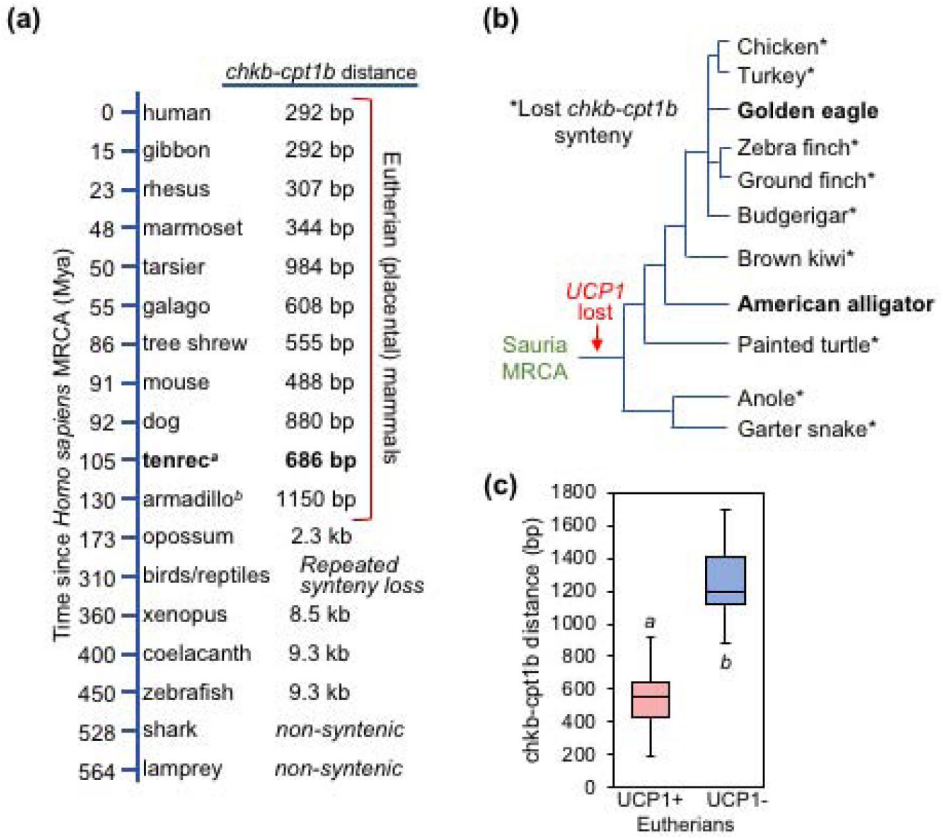

Figure 6. *Chkb-cpt1b* synteny is constrained by functional UCP1.

(a) Cladogram of *chkb-cpt1b* locus structure. *H. sapiens* MRCA (most recent common ancestor) divergence times were adapted from a molecular timescale of vertebrate evolution [79]. [a]Tenrec represents the oldest eutherian lineage in which canonical BAT has been shown to develop. [b]Armadillo lost the *UCP1* gene and is included in the data shown in panel (c). (b) Phylogenetic tree of *chkb-cpt1b* synteny in Sauria (extant birds and reptiles). Species that have lost *chkb-cpt1b* synteny are indicated by an asterisk, and species retaining *chkb-cpt1b* synteny are indicated in bold. UCP1 was lost in the saurian common ancestor [64]. (c) Box and whisker plot comparing the *chkb-cpt1b* intergenic distance in $UCP1^{+}$ and $UCP1^{-}$ eutherians (species listed in Materials and Methods). The intergenic distances were significantly different as determined by ANOVA ($P<0.05$).

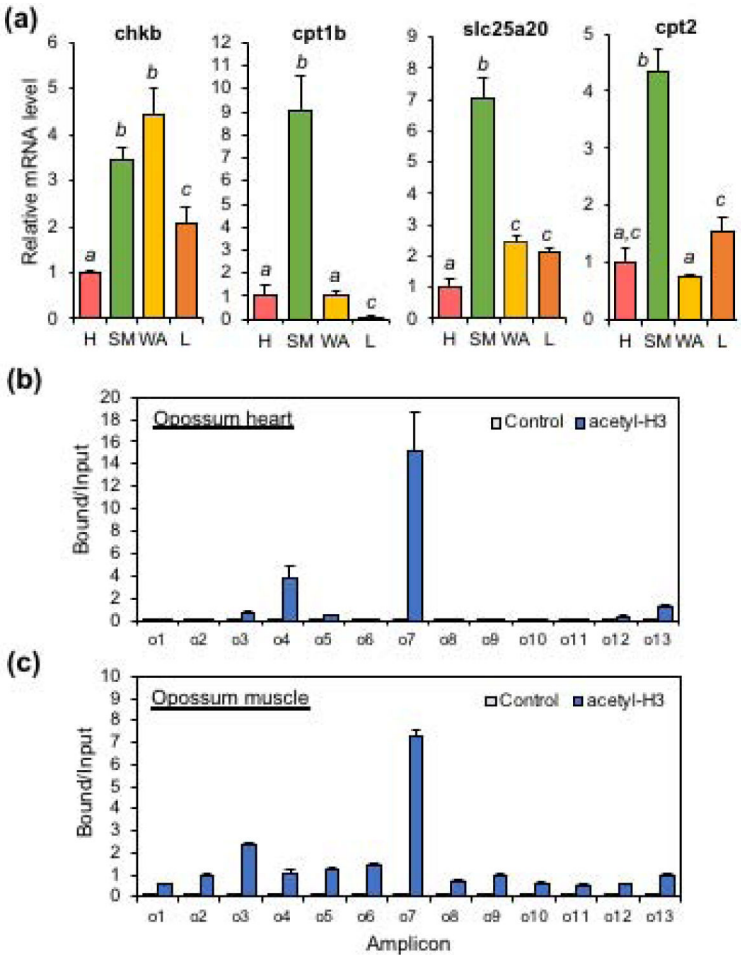

Figure 7. *Chkb* and *cpt1b* expression are unlinked in the opossum *M. domestica*.

(a) Tissue distribution of *chkb* and *cpt1b* transcription in opossum: heart (H), skeletal muscle (SM), white adipose tissue (WA), liver (L). Internally controlled mRNA levels (vs. *β2-microglobulin* mRNA) were normalized to the level in heart. Results of ChIP assays with a panacetyl-H3 antibody in opossum (b) heart and (c) skeletal muscle.

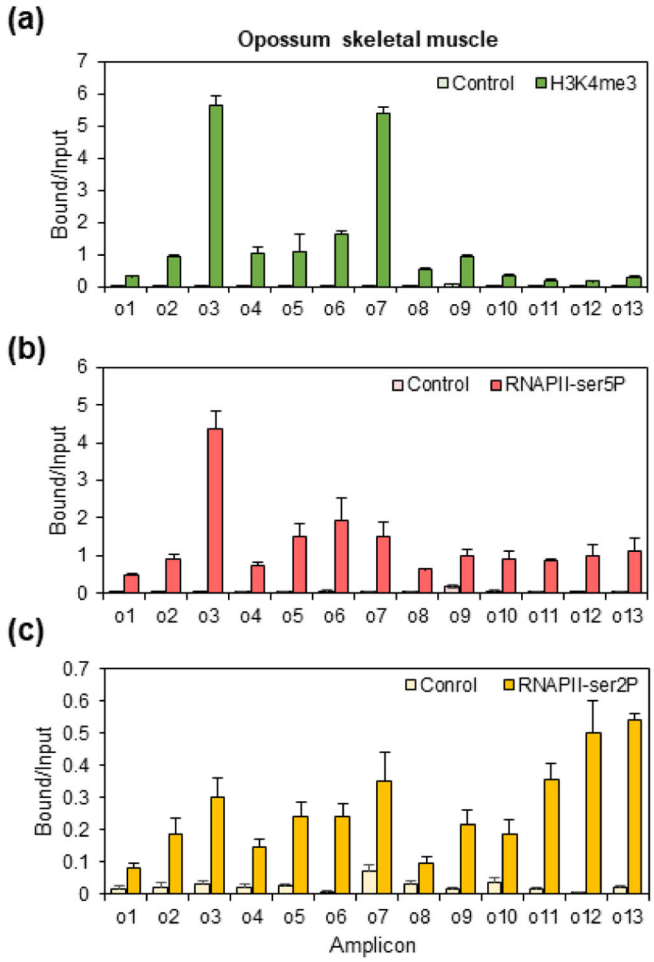

Figure 8. H3 lysine 4 trimethylation and RNAPII initiation are focused near the *Chkb* transcription start site and the *Cpt1b* 5' CGI in opossum skeletal muscle.

Results of ChIP assays. (a) H3 lysine 4 trimethylation. (b) RNAPII serine 5 phosphorylation (initiating form). (c) RNAPII serine 2 phosphorylation (elongating form). Amplicons are mapped in Figure 1c.

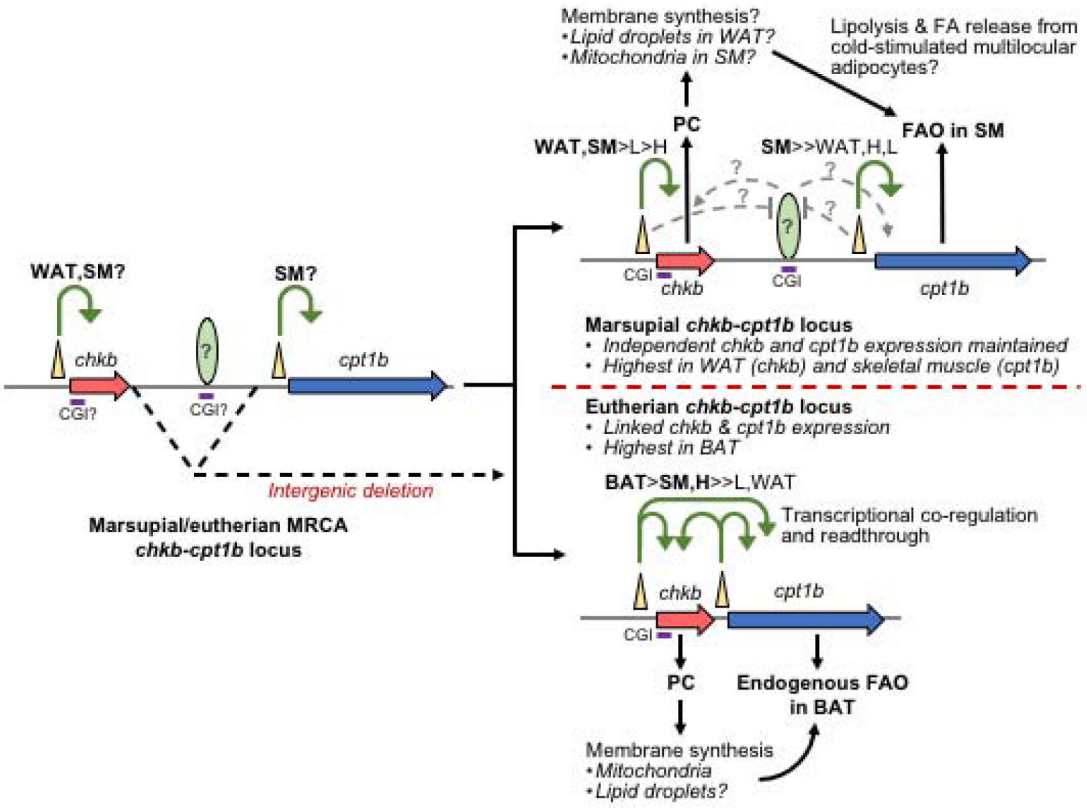

Figure 9. Model for the structural and functional divergence of the marsupial and eutherian *chkb-cpt1b* loci.

In the therian MRCA, the distally syntenic *chkb* and *cpt1b* genes were both expressed in skeletal muscle (SM), but only *chkb* was expressed in WAT as mediated by proximal elements (gold triangles, bent arrows). This pattern was maintained in marsupials due to the retention of the CGI associated with the marked peak of acetylation upstream of *cpt1b*, where putative regulatory complexes (green oval) may be insulating *cpt1b* from *chkb*-associated elements (gold triangles), and/or providing independent enhancer function (dashed arrows). In eutherians, the deletion of the intergenic CGI eliminated the associated putative insulator and/or activating function, allowing the regulation of *cpt1b* to be co-opted by *chkb*-associated sequences, with reciprocal crosstalk from *cpt1b*-associated elements, which resulted in novel co-expression of these genes in an adipocyte lineage that became BAT.

Table 1.

Primer sequences for mRNA quantification by qRT-PCR.

Transcript	Forward Primer	Reverse Primer
Mouse		
Chkb	TCCCTGAGATGAACCTGCTG	GGCGATGGGGTAGACTCTAG
Cpt1b	CAACTCCTGGAAGAAACGCC	TCCACCTTGCAGTAGTTGGA
Chkb-Cpt1b	CCCCACCTCAAGTTTCTCCT	TACTGCCTGGTGTGCTTCC
Cpt2	ACTAAGAGATGCTCCGAGGC	AACAAGTGTCGGTCAAAGCC
Slc25a20	CTCTGGGACCTTGGACTGTT	AAACCCAAAGAAGCACACGG
B2m	CCCTGGTCTTTCTGGTGCTT	CGTAGCAGTTCAGTATGTTCG
Opossum		
chkb	GCGCCTTTGGATAAGCTGAT	TGGTTCCCAATGTCAAAGCC
cpt1b	GGGGTAGACTTCCAGCTCAG	CATGACAACGACCAGCCAAC
cpt2	AGATACCTCAGTGCCCAGAG	CTTTCAAAGGACCGGCAGAG
slc25a20	ACTCTGGGACGTTTGACTGT	CCCCAATCCAAAGCCAAAGA
b2m	TTGTGCTTCCTTCCCTACCT	TGGAATCCTGACACGTAGCA

Table 2.

Primer sequences for ChIP assay fraction analysis by qPCR.

Amplicon	Primer Sequences	
m1	CCCACCTGCACGTTTATCTG	CACTGAGAGCTGGAGAGAGG
m2	CTCTTCAGCCCCATCCCTAG	GAAAGGGCCTCAAAGCTACG
m3	TAAACCTAACGGAGCCCACG	CATCCTGCAAACCGTCCTTG
m4	AGGTGCTGCTACGACTCTAC	TTGCTCCAGATGTCCGAACT
m5	ATTCCAATCTCCCCAGTCCC	CCTTCTGAACCTCTGCCAGA
m6	CTCCTGGTGACCTTTTCCCT	CACAAGGTTGCTGGAAGGTC
m7	GGCACACTAAGCACCTTCTG	CTCAGAGCCTCCCGACTAAG
m8	CTCAAGTCATGGTGGGCAAC	TCTTCCCACCAGTCACTCAC
m9	GAAGAGAGCCCATCCCTTGT	TGTCTAAGCCAGTCCCTGTG
m10	CGATAGGGCTCTGTGGGATT	TCTAACTTGCCCCTCCTTGG
m11	AAAGAGATACCCCAGCTGCC	CACTGCCTCAAGAGCTGTTC
m12	GATGCCTGTAGTGTGCAAGG	TCCCTTACTGAAGCCCTTGG
o1	ACCCATTCACCTCTCCCAAG	TGTGCTCAACCCTCTTCTCC
o2	GCCTCAGCCAAGAAAACCCT	TGGAAAGATGCCGAGGACTG
o3	ACGTGACCTATGAGCAGACG	CAGTCAGATACCCTCCGCAG
o4	CCGGCTTTATGGGGTCTTCC	ACTAAGGTGGGAGATTGGGG
o5	AAACAGGTAAAGGCCGAGGA	CCAGAGGCCCCAGAATATGT
o6	CACACCCAGATGTCTCCCCA	GTGTGAAGGTGGAGGGTACA
o7	GAAGGGTCTGAGGGTCTGTG	CAGCCAGCTTCAGGACAAAG
o8	GGACCTTTCTGCCCTCATCTA	CAGGAGCAGAAAGGAGCACT
o9	GTTGGCTGGTCGTTGTCATG	ATGCAGCAGATCATCCCCAT
o10	ATGTCATGGTAAGAGCCGGG	CGTCCCTGACTGTGACTTCT
o11	CGGAATGGATTTGGAGCTGG	CCTTGGATTTCAGCCTGCTC
o12	AGATCTTCCCTCCACCCTCT	CTGCTTTCTCGGTGGGGATA
o13	CCTCCTTCCTCTCAATGCCA	AGCTTGGCCCTAAACTCACT
h1	CCCCAGCCAGAATCAGTTTT	CTTGAACCCAGGCCTTGTTG
h2	GGAATGAATGAAGACGCGCA	TGCTGAAGGAATGTGACCCT
h3	GCGATGCGGGTAGTATTGTT	AGGCTTCGGTGTAATGAGGT
h4	TCCTGACTCTTGGCCATTGA	CCTTCCTCACCGACTGACTT
h5	ACATCGGTGACCTTTTCCCT	GGGTTTCTGTGCGGTGAAG
h6	GAGGCCCTGAAACACGTCTA	CTCTGGGAGAAGCACCTGTG
h7	CTCAAGTCATGGTGGGCAAG	GGGGAGGTGGAAGGTTAGAG
h8	TTCCCTGCTTCTGACACTGT	CTCTCACGCAACACCAACAA
h9	AAGTGTCCTCTGCCCATGTG	GCGGGGCAGAAGTAAAGG
h10	TTTTCCAAGTTCCCAAGGCC	GTGTCCTTGGAGCCTGGG
h11	GTGTCTGTTGAACACCCACC	CGACATGGGCAGGAATAGGA